Titration of Fatty Acids Solubilized in Cationic, Nonionic, and Anionic Micelles. Theory and Experiment

5 AUTHORS, INCLUDING:

Fernando Luís Barroso da Silva
University of São Paulo
24 PUBLICATIONS **355** CITATIONS

SEE PROFILE

Olle Söderman
Lund University
210 PUBLICATIONS **6,270** CITATIONS

SEE PROFILE

Titration of Fatty Acids Solubilized in Cationic, Nonionic, and Anionic Micelles. Theory and Experiment

Fernando Luís B. da Silva,*,[†,‡] Dan Bogren,[§] Olle Söderman,[§] Torbjörn Åkesson,[‡] and Bo Jönsson[‡]

*Departamento de Física e Química, FCFRP, Universidade de São Paulo, Av. do café, s/no.,
14040-903 Ribeirão Preto, São Paulo, Brazil, Department of Theoretical Chemistry, Lund University,
P.O. Box 124, S-221 00 Lund, Sweden, and Department of Physical Chemistry 1, Lund University,
P.O. Box 124, S-221 00 Lund, Sweden*

The titration properties of a fatty acid solubilized in different types of micelles, cationic, anionic and nonionic, have been investigated experimentally and theoretically. The solution containing micelles, counterions, and added salt was treated as a dielectric continuum in the Monte Carlo simulations. The dielectric permittivity of the interior of the micelle can have a profound effect on the calculated pK shifts depending on how the dielectric discontinuity is chosen in the model. The simulated results are compared to data from Poisson—Boltzmann calculations and from experiments. The experimentally observed apparent pK_a value changes from 7.6 to 4.9 when solubilizing lauric acid in anionic (SDS) and cationic (DoTAC) micelles, respectively. For the nonionic micelle it is found to be approximately 6.6. A significant ion specificity in the pK_a value is observed for the DoTAC and DoTAB systems and surprisingly enough both systems show an upward pK shift.

I. Introduction

Almost all industrial processes involve colloidal systems and often charged amphiphilic molecules. There is consequently a strong interest to understand and control the colloidal stability, which depends among other things on the surface potential of the colloidal particles. Thus, much interest has focused on the measurement of the electrical potential at the interface between the aqueous solution and the aggregate core.[1−7] After the classical works of Mukerjee and Banerjee[1] and Fernandéz and Fromherz,[2] a typical experimental approach has been to employ interfacially located acid−base indicators and to obtain the mean electrostatic potential (ϕ) from the equation

$$pK_a^{obs} = pK_a^0 - \frac{F\phi}{RT \ln 10} \qquad (1)$$

where pK_a^{obs} is the measured pK_a, pK_a^0 is the intrinsic interfacial dissociation constant of the probe, F is the Faraday constant, R is the universal gas constant, and T is the absolute temperature. The apparent simplicity of this equation hides several fundamental problems: (i) a correct measurement of pK_a^0, (ii) the location of the probe, and (iii) the importance of nonelectrostatic interactions.

The meaning of the intrinsic interfacial dissociation constant is that it should be the acid constant of the probe in the presence of the interphase but in the absence of any electrostatic interactions. This is a somewhat obscure and artificial property and its accurate determination is a nontrivial experimental task.

The problem has sometimes been circumvented by assuming that pK_a^0 would be equivalent to the pK_a value obtained in pure water, pK_a^w.[1] However, recent studies have indicated that this is not always the case.[2−6] Instead, experiments with nonionic micelles are usually performed and believed to give better estimates of pK_a^0.[2−7] Although questionable and still an unsolved problem, the latter seems to be the more common approach today.

Ideally, the probe should have a size compatible with the surfactants and reside, on the average, in the plane of the charged surfactant headgroups, i.e., at the interface. Available data in the literature for different probes indicates that their location may not always be at the interface.[4−6] In addition, rather bulky dye molecules are often used, the perturbation of which on the micelles is probably quite substantial. In this work, we have chosen to use a fatty acid probe molecule of the same hydrocarbon chain length as the surfactant. The probe concentration is adjusted so that each micelle will contain, on average, one probe molecule. The pK_a values of the solubilized probe have been determined from pH titrations and are compared with the corresponding data obtained from theoretical modeling.

Theoretical attempts to study such systems are predominantly done using the dielectric continuum model, where only solute molecules enter explicitly in the model. The solvent is taken into account in an average way via a uniform permittivity, ϵ_s.[8] Spherical micelles are usually modeled by charged hard-spheres, whose interiors have a dielectric constant of ϵ_m. Often micelle−micelle interactions are not fully taken into account and just a single micelle is placed in the center of a spherical cell together with its counterions and added salt. This is referred to in the literature as the *cell model*.[9−11]

To solve such an *effective* Hamiltonian model, analytical or numerical calculations may be performed. A widely used

---

* Author to whom correspondence should be addressed. Phone: +55 (16) 602 4219. Fax: +55 (16) 633 2960. E-mail: fernando@fcfrp.usp.br.
† Universidade de São Paulo.
‡ Department of Theoretical Chemistry, Lund University.
§ Department of Physical Chemistry 1, Lund University.

approach is by means of the Poisson−Boltzmann (PB) theory.[10−12] This is a mean-field approximation that neglects ion−ion correlations, and treats the free ions (counterions and added salt) as point-charges. Alternatively, one may carry out computer experiments (Monte Carlo or Molecular Dynamics simulations), where the model can be solved exactly within the statistical errors. There are several examples of Monte Carlo (MC) calculations used to characterize micelle systems.[13−15] Except for ref 15, these studies are carried out with the common assumption that $\epsilon_m = \epsilon_s$. This is clearly an approximation and the micelle interior might have a static dielectric constant significantly lower than the solvent. The question is whether in a macroscopic continuum model, there is any need for introducing a dielectric interface ($\epsilon_m < \epsilon_s$) to describe pK_a shifts. This is one important topic of the present paper.

With this in mind, we construct a theoretical model for prototropic molecules in self-assembled surfactant aggregates suitable for computer simulations. This model includes the possibility to treat the micelle interior as a low dielectric medium. It is by no means clear that the introduction of a dielectric discontinuity means a refinement of the uniform case. In fact, we have already demonstrated that there is no gain including a dielectric interface when studying salt pK shifts for protein models.[16,17] Furthermore, a macroscopic model with a dielectric interface requires two additional parameters not known a priori: (i) an appropriate choice of the dielectric constant for each medium, and (ii) the location of the dielectric discontinuity.

The first issue has been a matter of intense controversy and debates in the literature, in particular, in a biologically oriented context.[18−21] In general, numbers in the range of 2−8 are used for the interior dielectric permittivity, ϵ_m. Some authors employ a value of 2 for the macromolecule, when there is no reorientation of fixed dipoles and/or charges within the molecule, whereas values of 4−6 are used for systems with some reorientation of dipoles.[22] Other alternatives with larger values have also recently been suggested.[23−27]

The location of the dielectric boundary is another problem, since it is far from clear where it should be placed. The dielectric constant is a macroscopic property that depends on the material organization at the microscopic level. Thus, the transition between two media is not discontinuous, but a smooth transition that extends a few angstroms inside each medium is a more realistic picture. Moreover, the interfacial region may have a dielectric behavior neither equivalent to the micelle core nor to the aqueous solution phase. The dielectric permittivity might also undergo changes upon proton binding.

Besides these uncertainties, a dielectric discontinuity also requires a consistent set of equations in order to describe the dielectric boundary. This introduces computational complications and substantially increases the computational costs. Hence, there should be an improvement in the results in order to follow such complex and demanding prescription.

II. Theoretical Modeling

The classical theoretical representation of a micelle is a perfect rigid sphere with uniform surface charge density. The surfactant headgroups charges are taken into account only as smeared out charges at the micellar surface, neglecting their discrete nature. Here we propose a slightly more realistic model that resembles Stigter's view,[28] where the headgroups of the prototropic molecule and the surfactants are explicitly introduced. A schematic picture of the model for a negatively charged micelle is given in Figure 1. The headgroups are modeled as hard-
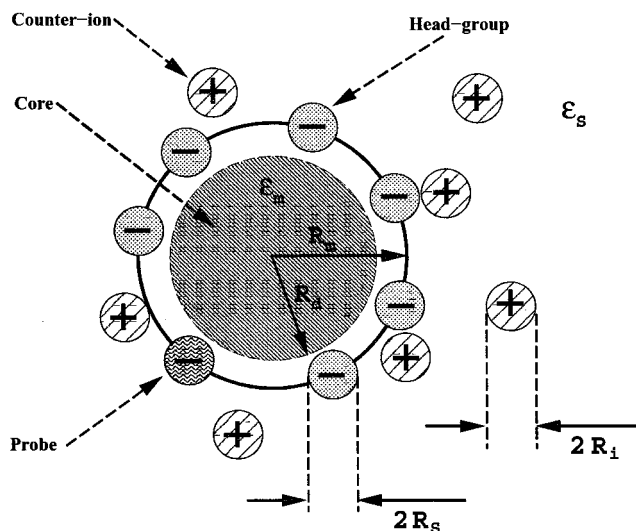

Figure 1. Schematic representation of an anionic micelle. The surfactant headgroups and the probe are located at the micelle surface, a distance R_m from the center. The low dielectric cavity of the micelle core has a radius of R_d and a dielectric constant of ϵ_m.

spheres of radius R_s with a central charge z_s. These spheres are kept at a distance R_m from the aggregate center and are free to move on this surface. The total number of headgroups, N_{ag}, is assumed to be constant and equal to 67 in order to mimic a typical C_{12} surfactant. In addition, a single prototropic molecule is placed in the micelle. Its headgroup is assigned a hard-sphere radius equal to the surfactant headgroups, and a charge of $z_p = -1$, which is positioned a distance R_m from the micellar center. The core of the micelle is represented by a concentric spherical cavity of radius R_d (referred to as the dielectric interface radius) with a dielectric permittivity ϵ_m. Surrounding the micelle is an aqueous electrolyte solution described by the so-called restricted primitive model.[29] Each ion i with valence z_i is treated as a hard sphere of radius R_i, while the solvent degrees of freedom are characterized by an average dielectric permittivity $\epsilon_S \neq \epsilon_m$ that is also assigned to the ionic interior. All charges are assumed to be in the high dielectric medium.

As usual, the entire system (micelle and free ions) is confined to an electroneutral cell of radius R_c, the value of which defines the micellar concentration. The electrostatic interactions for this system may be developed by means of a multipole expansion in terms of Legendre polynomials.[30] These power series are not ideally suited for numerical simulations, due to the need of a large number of terms for a convergent calculation. This is particularly problematic when charges are lying close to the dielectric boundary. However, if the charges are more than ≈ 0.3 Å from this boundary, it is feasible to perform such calculations and use the Legendre polynomials in an MC simulation,[17] although the computational burden increases by one or 2 orders of magnitude compared to assuming a uniform dielectric permittivity.

According to Böttcher,[30] the electrostatic energy for two ionized sites of valence z_i, z_j located at radial positions r_i, r_j (r_i and $r_j > R_d$) and subtending an angle θ_{ij}, is given by

$$u^{el}(r_{ij}) =$$
$$\frac{z_i z_j e^2}{4\pi\epsilon_0\epsilon_s}\left(\frac{1}{r_{ij}} + \frac{1}{R_d}\sum_{n=1}^{n_{max}}\frac{(\epsilon_s - \epsilon_m)P_n(\cos\theta_{ij})}{(\epsilon_s(1 + 1/n) + \epsilon_m)}\left(\frac{R_d^2}{r_i r_j}\right)^{n+1}\right), \begin{cases} r_j > R_d \\ r_i > R_d \end{cases}$$

$$(2)$$

where e_o is the vacuum permittivity, $r_{ij} = [r_i^2 + r_j^2 - 2r_ir_j \cos \theta_{ij}]^{1/2}$ is the spatial separation, e is the elementary charge, P_n is the Legendre polynomial of order n, and n_{max} is the maximum number of terms included in the sum. The first term in this equation is the direct Coulomb interaction, while the second describes the reaction field accounting for the induced polarization charge at the dielectric discontinuity. For a uniform dielectric medium ($\epsilon_m = \epsilon_s$), eq 2 reduces to the ordinary Coulomb energy,

$$u^{el}(r_{ij}) = \frac{z_iz_je^2}{4\pi\epsilon_0\epsilon_s r_{ij}} \tag{3}$$

Combining the electrostatic interactions with a short ranged hard-core potential $u^{hs}(r_{ij})$ to prevent Coulomb collapse in the Markov chain, the full configurational energy of the system $U(\{\mathbf{r}^N\})$ then becomes

$$U(\{\mathbf{r}^N\}) = \sum_{i=1}^{N_c + N_S} v^{ex}(r_i) + \frac{1}{2}\sum_{i=1}^{N}\sum_{j=1}^{N}(u^{el}(r_{ij}) + u^{hs}(r_{ij})) \tag{4}$$

where $N = N_c + N_s + N_{ag}$ is the total number of charges comprising N_c mobile counterions, N_s mobile added salt ions, N_{ag} charged surfactant molecules, and $u^{hs}(r_{ij})$ is given by

$$v^{hs}(r_{ij}) = \begin{cases} \infty, & r_{rj} \leq (R_i + R_j) \\ 0, & \text{otherwise} \end{cases} \tag{5}$$

The term $v^{ex}(r_i)$ is an external potential that imposes the cell boundary and the micellar surface constraints,

$$v^{ex}(r_i) = \begin{cases} 0, & (R_i + \max\{R_m, R_d\} \leq r_i \leq R_c) \\ \infty, & \text{otherwise} \end{cases} \tag{6}$$

Numerical Simulations. Within the cell model approach, the micelle center remains fixed at the center of the electroneutral cell during the calculations. The results presented here were obtained with cell radii of $R_c = 51.4$, 40.9, and 35.8 Å, which approximately corresponds to surfactant weight fractions, w_f, of 0.05, 0.10, and 0.15, respectively. In most of the simulations, the micelle radius R_m was set to 19 Å, a typical average value for a C_{12} ionic surfactant micelle. Three different spherical systems were studied: a cationic, a neutral, and an anionic micelle. Unless otherwise stated, the probe, the headgroups, and the mobile ions were assigned a common hard-core radius of 2 Å. The influence of the aggregation number on the outcome was also tested.

The dielectric boundary was placed at different locations by a change of the dielectric cavity radius R_d. Numbers ranging from the uniform dielectric case ($R_d = 0$) to the nonuniform case with the boundary up to 0.3 Å from the micelle surface were used. The dielectric constant for the low dielectric cavity was taken to be $\epsilon_m = 2$, which is a typical value for a hydrocarbon medium. The rest of the system was assumed to have a dielectric constant of $\epsilon_s = 78.7$.

Equilibrium configurations were sampled from the canonical (NVT) ensemble generated by the standard Metropolis Monte Carlo algorithm.[31,32] The temperature was fixed at $T = 298.15$ K and 100 000 simulation cycles were used to collect the final data after the initial equilibration, except for the neutral micelle case where 10 times longer simulations were employed. The results were compared with Poisson−Boltzmann calculations[10,33] for a smeared out charge micelle model.

Free Energy Calculations. Consider the dissociation of an acid (HA),

$$HA \rightleftharpoons H^+ + A^- \tag{7}$$

At equilibrium $\Delta G = 0$ and when written in terms of the corresponding chemical potentials and activities, $\mu = \mu_o + kT \ln a$, the condition reads,

$$\mu_H + \mu_A - \mu_{HA} = \mu_H^o + kT \ln a_H + \mu_A^o + kT \ln a_A - (\mu_{HA}^o + kT \ln a_{HA}) = 0 \tag{8}$$

where k is Boltzmann's constant. Introducing the *thermodynamic* binding constant, K, one obtains the familiar form,

$$\Delta G^0 = -kT \ln K = -kT \ln\frac{a_Ha_A}{a_{HA}} \tag{9}$$

Many experiments involve a *stoichiometric* binding constant, K^s,

$$K = \frac{a_Ha_A}{a_{HA}} = \frac{c_Hc_A}{c_{HA}}\frac{\gamma_H\gamma_A}{\gamma_{HA}} = K^s\frac{\gamma_H\gamma_A}{\gamma_{HA}} \tag{10}$$

where the c's stand for concentrations and the γ's are activity coefficients. Since the thermodynamic binding constant is a true constant, any change in K^S is a measure of a change in the activity coefficients. In a typical titration experiment, one measures the amount of acid or base and pH. In the following we will assume that pH $= -^{10}log\ a_H$. Thus, the resulting quantity is usually a mixed stoichiometric and thermodynamic binding constant like

$$K = \frac{a_Hc_A}{c_{HA}}\frac{\gamma_A}{\gamma_{HA}} = K^s\frac{\gamma_A}{\gamma_{HA}} \tag{11}$$

It is convenient to choose a reference state with a corresponding stoichiometric binding constant, K_{ref}^S, and to measure any changes relative to this state. Let us also introduce the notation $\mu^{ex} = kT \ln \gamma$, which allows us to write the dissociation constant *shift* as

$$\Delta pK^S = -^{10}log\frac{K^S}{K_{ref}^S} = \frac{(\Delta\mu^{ex} - \Delta\mu_{ref}^{ex})}{kT \ln 10} \tag{12}$$

where $\Delta\mu^{ex} = \mu_A^{ex} - \mu_{HA}^{ex}$ is the change in excess free energy for the binding process. We will assume that the excess part is dominated by electrostatic interactions and that other contributions, including structural changes, solvation, etc., are either small or independent of added salt or other modifications of the electrostatic interactions. In the latter case they will cancel when calculating ΔpK^s. From a computational point of view it is advantageous to introduce the excess chemical potential of the bound proton as $\mu_B^{ex} = \mu_{HA}^{ex} - \mu_A^{ex} = -\Delta\mu^{ex}$.

Up to this point the derivation has been quite general, but let us now choose the reference state as the free acid in pure water. In this case all the excess chemical potentials can be set to zero and eq 12 can be written as

$$RT \ln 10\Delta pK^S = \mu_{A(mic)}^{ex} - \mu_{HA(mic)}^{ex} = -\mu_{B(mic)}^{ex} \tag{13}$$

where $\mu_{B(mic)}^{ex}$ is the excess chemical potential of a proton bound to the amphiphilic probe in a micelle. The excess free energy of a bound proton can be straightforwardly obtained in

a MC simulation by means of a modified Widom's test particle insertion method.[34]

In the mean field approximation one obtains the electrostatic potential directly when solving the Poisson−Boltzmann equation. One usually makes the assumption that the potential ϕ is equal to the potential at the micellar surface and this is the procedure followed in this work. An alternative way is to perform two PB calculations, one with the probe ionized and another with it neutralized. The free energy difference between these two systems is then the desired free energy difference. Experience has, however, shown that the two routes give roughly the same result.

III. Experiments

Materials. The anionic surfactants, sodium dodecyl sulfate (SDS) and lithium dodecyl sulfate (LDS), used in the experiments were supplied by Sigma, St. Louis. The cationic surfactants, dodecyltrimethylammonium chloride (DoTAC) and dodecyltrimethylammonium bromide (DoTAB), were purchased from Kasei, Tokyo, Japan. The nonionic surfactant n-dodecyl-octaoxyethyleneglycomonoether ($C_{12}E_8$) was obtained from Nikko Chemicals, Japan. They were used as received.

The prototropic molecule, lauric acid ($C_{12}H_{24}O_2$), was from Acros organics, New Jersey, and a GC reference product. Sodium hydroxide (NaOH), analytical grade, and acetic acid (99.8%) were obtained from MERCK, Germany. The aqueous solutions were prepared using Millipore filtered water (conductivity $<10^{-6}\ \Omega^{-1}\ cm^{-1}$). The samples were prepared by weighing appropriate amounts of surfactant, lauric acid, and boiled Millipore water into glass tubes, which were immediately sealed off. They were stirred vigorously and heated in a water bath until a clear solution was obtained. The ratio of the number of surfactant molecules compared to the number of solubilized lauric acid molecules is chosen to be about 60:1. Therefore, there should be on the average one lauric acid molecule in each micelle, considering the aggregation number of these micelles.

We have assumed that the micelles remain spherical up to the highest concentration used (15 wt percent corresponding to approximately 0.5 M for the C_{12} surfactants used). For SDS, Croonen et al.[35] showed by fluorescence techniques that the aggregation number of SDS is around 80 at 0.5 M and thus SDS remains approximately spherical even at the highest concentration used here. Johansson and Söderman[36] showed that the same state of affairs holds for DoTAC. For DoTAB, we note that the macroscopic viscosity of the 15% sample is quite low (roughly the same as the corresponding DoTAC solution), which would indicate that also the DoTAB micelles remain approximately spherical.

pH-Titration Experiments. The pH values were determined by using a Radiometer Copenhagen PHM 210, which was calibrated by employing Radiometer buffer solutions. The pH-meter was calibrated before and after the experiments with pH 4 and pH 10 buffer solutions. No deviation in the calibration was detected, when comparing the results before and after the experiments. The titrations were carried out in a dynamic mode with increments of added NaOH varied according to the rate of the pH change, and were stopped when the pH reached 10. The temperature was not regulated in the experiments, but it was measured each time and was typically about 25 °C.

Titrations were performed for a series of surfactant solutions with different concentrations ranging from 5 to 15 wt % surfactant. Several control experiments were performed in order to ascertain that the influence of the surfactant on the glass electrode is negligible. Titrations of acetic acid with NaOH in
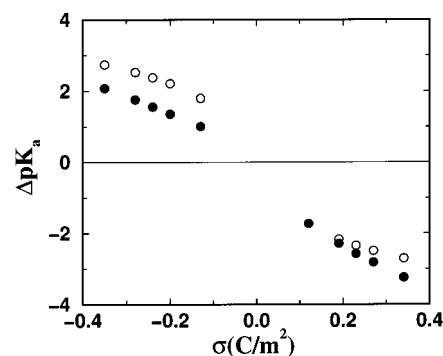

Figure 2. The Monte Carlo and Poisson−Boltzmann calculated ΔpK as function of the micelle surface charge density. Calculations were done with $\epsilon_m = \epsilon_s$ at $w_f = 0.05$. The MC standard deviation is estimated to be 0.02. Filled and open circles represent MC and PB results, respectively.

the absence and presence of both anionic and cationic surfactants below cmc gave the same pK_a, as did titrations in the presence of anionic surfactant at concentrations above cmc. The obtained pK values were in all these control experiments equal to 4.8. The data from the pH-titration experiments were analyzed with a least-squares routine using the Lewenberg−Marquardt algorithm.[37] The protocol yields values for pK_a and the (known) initial amount of added acid to the sample. The latter quantity was used as a control of the procedure. The obtained quantity of acid never deviated by more than three percent than the weighed amount.

IV. Results and Discussion

The outline of this section is as follows. We start by discussing results from the theoretical approach and how these are affected by variations in surface charge density, micellar concentration, the inclusion of a dielectric boundary, and counterion specificity. We then proceed to discuss the experimentally determined pK values, which are compared to the calculated ones. Finally we end with some concluding remarks.

Surface Charge Density. The distribution of counterions varies with the surface charge density, $\sigma = N_{ag}/4\pi R_m^2$. Micellar aggregation numbers, N_{ag}, are average numbers with an experimental uncertainty of a few percent. Hence, we have investigated how σ affects ΔpK. Figure 2 reports the MC and PB values of ΔpK for anionic and cationic micelles with different σ's, that is the aggregation number is changed but the micellar radius, R_m, is kept constant. A change of about 10% in σ at a typical micellar charge density only changes ΔpK by 0.15 pK units for both micellar systems. Similarly, if the aggregation number is kept fixed and the R_m is changed by 1 Å then the acid constant changes by ca. 0.1 pK units.

The Poisson−Boltzmann equation describes the trend in an almost quantitatively correct way, although it does not capture the slight asymmetry of the simulated ΔpK's. In the simulations with an anionic micelle, the probe in its ionized form will try to avoid the negative headgroups and when solubilized in a cationic micelle it will try to accumulate surfactants. This type of correlation between charges is absent in the Poisson−Boltzmann treatment. In general, correlations between oppositely charged species are more important than between charges of the same sign. Correlations between the probe molecule and the counterions are also more important than correlations with the surfactant headgroups, since the latter are restricted to remain on the micellar surface.

The Dielectric Boundary. The model is sensitive to the choice of dielectric radius R_d, if it is close to the micellar radius

TABLE 1: ΔpK Obtained from Poisson−Boltzmann Calculations (ΔpK_{PB}) and Monte Carlo Simulations (ΔpK_{MC}) as a Function of the Weight Fraction Surfactant (w_f)[a]

micelle	w_f	ΔpK_a^{obs}	ΔpK_{PB}	ΔpK_{MC} data for different R_d				
				0.0	17.0 Å	18.5 Å	18.67 Å	18.7 Å
anionic	0.05	2.8	2.38	2.21	2.22	2.94	3.59	3.80
	0.10	2.4	2.03	1.86	1.86	2.58	3.25	3.46
	0.15	2.4	1.80	1.64	1.65	2.37	3.03	3.24
neutral	0.09	1.9	0.0	0.06	0.17	1.18	1.89	2.13
cationic	0.05	0.1	−2.44	−2.68	−2.50	−1.31	−0.53	−0.31
	0.10	0.6	−1.99	−2.35	−2.18	−0.99	−0.20	0.03
	0.15	1.0	−1.76	−2.13	−1.97	−0.77	0.02	0.24

[a] Five different low dielectric radii were studied (R_i = 2 Å). Experimental results, $\Delta pK_a^{obs} = pK_a^{obs} - pK_a^w$, for SDS, $C_{12}E_8$, and DoTAC are included for comparison. Surface charge density is assumed to be 0.23 C/m^2.

R_m. This may be seen in Table 1, where ΔpK is calculated for R_d values ranging from zero to 18.7 Å. The presence of the dielectric interface gives rise to large energies for charges located very close to the interface, this is the so-called "image-charge effect". Hence, neutralizing a negative probe sitting in a micelle causes a significant change in electrostatic energy. This is a favorable process and the effect becomes really significant for probes residing close to the dielectric discontinuity, i.e., probes that are partially desolvated−see Table 1. The image term will eventually diverge when $R_d = R_m$. For instance, proton binding to an anionic micelle is several times more favorable, when the micelle has $R_d = 18.7$ Å as compared to $R_d = 0.0$ Å. For a probe in a positively charged micelle, the effect can also change the sign of ΔpK. This is the case, for instance, when $R_d = 18.7$ Å at $w_f > 0.05$. In a neutral micelle, ΔpK is essentially only measuring the self-image contribution of the electrostatic interaction.

This sensitivity of the model is of course a weakness as we have really no firm ground for choosing the radius of the low dielectric sphere of the micelle. One viable way, although not completely unambiguous, is to use the nonionic micelle as a reference for estimates of R_d. The problem is that we do not know where the probe is situated in a nonionic micelle. The outer layer contains a significant fraction of EO-groups, which will change the dielectric permittivity of the region and it may be a rather crude approximation to assume this region to be "water-like". Keeping these problems in mind, we will still use this route as an alternative way for interpreting and comparing our results.

Another way to interpret the results is to focus on the difference in ΔpK between a cationic and an anionic micelle. This is a much safer but, unfortunately, also less informative approach.

The counterion distribution around the micelle was calculated from the Monte Carlo simulations. The presence of a dielectric boundary, i.e., $\epsilon_m \neq \epsilon_s$ tends to decrease the number of counterions close to the micelle, but the effect is marginal[15] − see Figure 3.

Micellar Concentration. Table 1 also summarizes the micellar concentration effects in the pK shifts. Increasing the surfactant concentration and hence the micelle concentration, leads to a stronger screening of the electrostatic interactions and one should expect to see a decreasing magnitude of ΔpK for both cationic and anionic micelles. This is indeed what is found and a 3-fold increase in surfactant concentration reduces ΔpK by approximately half a pK unit. One can note that this shift is independent of R_d, since the image charge contributions at the two densities are approximately equal and hence cancel.
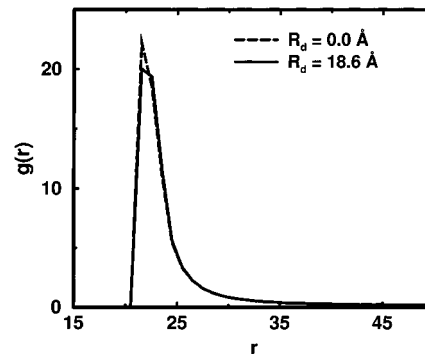

Figure 3. Radial distribution function for counterions around a negatively charged micelle. Comparison between the uniform and nonuniform dielectric case for $\sigma = -0.35$ C/m^2.

TABLE 2: Simulated pK Shifts as a Function of the Counterion Size[a]

micelle	R_d Å	MC results for R_i		
		1 Å	2 Å	3 Å
anionic	0.0	1.77	2.21	2.64
	18.5	2.54	2.94	3.34
	18.67	3.21	3.59	4.02
cationic	0.0	−2.30	−2.68	−3.08
	18.5	−0.97	−1.31	−1.69
	18.67	−0.20	−0.53	−0.89

[a] Data for $w_f = 0.05$, $R_m = 19$ Å, $R_d = 0$, and $\sigma = 0.23$ C/m^2.

A comparison between MC and PB data shows good agreement in this respect, which is a result of cancellation of both image and correlation terms. The agreement with experimental data is also good both for anionic and cationic micelles. A similar behavior has been seen for titrating groups in proteins, where the effect of changes in protein concentration and protein charge (via mutations) are correctly reproduced in MC simulations.[38]

Counterion Specificity. Changing the ionic radius is a rough manner to introduce ion specificity. Table 2 reports ΔpK shifts obtained in MC simulations with different ion radii ranging from 1 to 3 Å. The main effect of increasing the radii is that the counterions are pushed away from the micelle and the electrostatic interactions between the headgroups become less screened. The absolute magnitude of the pK shifts when increasing the ionic radius from one to three Å is about 0.8 pK units and the result is virtually independent of the dielectric radius.

Experimental Results. Before presenting the results of the determination of pK_a values for lauric acid in micelles, it is appropriate to discuss the use of glass electrodes in pH determinations, in particular in surfactant solutions. There has been a debate in the literature recently concerned with what is actually measured with a pH electrode. Bunton and Yatsimirsky[39] maintain that the antilogarithm of pH is neither equal to the proton activity nor the concentration. In the following comparison between experimental and theoretical results, we have taken the point of view that the reading of the glass electrode is a measure of the activity of the hydronium ions. Besides this fundamental problem, the pH may also be influenced by systematic errors caused by the presence of (surface active) surfactants. As noted above, the control experiments performed here do not indicate any significant influence due to the presence of surfactant molecules. We also note that an error by a factor of 2 in the activity translates into an error in pH by only 0.3. Under the assumption that the pH value obtained from the glass electrode is related to a_H, the obtained pK_a value (from pH and the concentration of added base) corresponds to the dissociation constant as defined by eq 11.

TABLE 3: Experimental Data for the pH-Titration of Lauric Acid in Different Micellar Systems[a]

surfactant	w_f	c_{probe}	pK_a^{obs}	ΔpK_a^{obs}	ΔpK_1^{calc}	ΔpK_2^{calc}
SDS	0.05	2.7	7.6	2.8	2.21	3.59
	0.10	6.0	7.2	2.4	1.86	3.25
	0.15	8.5	7.2	2.4	1.64	3.03
LDS	0.05	4.1	7.6	2.8	2.21	3.59
	0.15	9.9	7.4	2.6	1.64	3.03
$C_{12}E_8$	0.09	2.3	6.6	1.9	−0.06	1.89
	0.27	10.0	6.7	2.0	−0.06	2.03
DoTAC	0.05	3.0	4.9	0.1	−2.68	−0.53
	0.10	6.4	5.4	0.6	−2.35	−0.20
	0.15	8.2	5.8	1.0	−2.13	0.02
DoTAB	0.05	3.4	5.7	0.9	−2.68	−0.53
	0.10	6.6	6.0	1.2	−2.35	−0.20
	0.15	6.8	6.2	1.4	−2.13	0.02

[a] c_{probe} corresponds to the amounts of lauric acid and is given in mM units. The experimental error is estimated to be 0.1 pK units. $\Delta pK_a^{obs} = pK_a^{obs} - pK_a^w$, and ΔpK_1 and ΔpK_2 refer to MC calculations with $R_d = 0$ and 18.67 Å, respectively.

For the sake of convenience, the main experimental results for the pH-titration are summarized in Table 3 together with MC data already listed in Table 1. The intrinsic interfacial pK_a of lauric acid in the nonionic micelle (pK_a^n) and in pure water (pK_a^w) were used as references for estimating the pK shifts in the charged micelles. The pK_a^w value is not available in the literature, but from ref 40 one finds that the acid constants in pure water for acetic acid, propanoic acid, and butanoic acid are close to 4.8 and change little when the carbon chain length is increased. For example, the pK_a^w for octanoic acid below the critical micelle concentration has been determined by ^{13}C NMR and found to be 4.85.[41] Therefore, we have assumed that pK_a^0 is equal to 4.8. The pK_a^n value was measured in the experiments and found to be 6.6 and approximately independent of the micellar concentration. Assuming that the probe molecule resides in a water-like environment one might attribute the shift from 4.8 to 6.6 as being solely due to the image charge effect of the probe itself, see below.

The observed pK_a value of lauric acid in an SDS micelle is about one pK unit higher than in the nonionic micelle. This can be understood qualitatively as a result of the electrostatic repulsion between the ionized probe and the negatively charged headgroups. Similar results are found for the LDS system. In the opposite case, in a cationic DoTAC micelle, the shift is 1.7 units smaller than in the nonionic case. This seems reasonable, since in this case there is a strong attraction between the probe and the cationic surfactants. We stress that these conclusions are based on the assumption that the nonionic surfactant is a good reference for estimating the image term.

A significant difference was found between DoTAC and DoTAB micelles. Although there might be some counterion specificity, the difference is apparently higher than what is commonly seen in experiments.[4−6] As a control experiment the dissociation constant of acetic acid was measured in five weight percent solutions of NaCl and NaBr. No deviations from the salt-free case were observed.

Finally, we note that experiments with tetradecanoic acid as the fatty acid probe in SDS and DoTAC yield the same results as with dodecanoic acid as probe (within the experimental uncertainties). One might argue that if the fatty acid probe were longer than the surfactant, then the carboxylic group would extend out in the water medium and thus be less affected by the presence of the surfactant film. This does not seem to be the case; the carboxylic acid headgroup appears to be solubilized in close proximity to the surfactant/water interface.

TABLE 4: Adding an Attractive Polarizability Term to the Ionic Interactions[a]

		calculated ΔpK for different u_a^C/kT				
exp.	interaction type	0.00	−0.25	−0.75	−2.00	−2.25
0.1/0.9	surf(+)-probe(−)	−2.68	−2.71	−2.79	−2.97	−3.01
	probe(−)-ion(−)		−2.67	−2.65	−2.58	−2.57
	surf(+)-ion(−)		−2.62	−2.50	−2.11	−2.03
	ion(−)-ion(−)		−2.67	−2.62	−2.50	−2.48

[a] u_a^C/kT is the value of the polarization term u_a at contact. Data for a cationic micelle with $R_d = 0$ at $w_f = 0.05$.

Model Predictions versus Experimental Results. The assumption behind the ΔpK data in Table 3 is that pK_a^0 is equivalent to the pK_a value obtained in pure water. With this assumption it is obvious from the data that a uniform dielectric model is unable to quantitatively reproduce the experimental numbers. A model with a dielectric discontinuity, however, requires as input a dielectric radius R_d, which is not known a priori. One possible alternative is to consider the nonionic micelle, $C_{12}E_8$ as an oil droplet of radius R_m dissolved in water and to neglect effects from the EO-groups on the dielectric permittivity close to the hydrocarbon part of the micelle. Assuming that the probe resides at the interface, then the only electrostatic effect is the image term of the ionized probe. Hence, we can use the experimental ΔpK from the nonionic micelle in order to determine R_d. With $R_d = 18.67$ Å simulations reproduce the experimental shifts for $C_{12}E_8$. Keeping this parameter fixed, calculations were repeated for other micellar systems and a reasonable agreement for both anionic and cationic micelles was found. However, the agreement is not significantly better than for the uniform dielectric model. An interesting observation was made by Spooner et al. who measured the titration behavior of long chain carboxylic acid solubilized in neutral emulsion and chylo-microns and consistently found an upward shift with to 7.3−7.6,[42] which is very close to the value found in our charged SDS micelles.

SDS and LDS give the same result within the experimental errors. For DoTAC and DoTAB there is a surprising difference in the measured ΔpK's. From the polarizabilities[43] of bromide and chloride ions one would expect to see a stronger screening of the headgroups by the former ion. This is indeed seen in the experiment where $pK_a^{Cl} < pK_a^{Br}$. The difference in ΔpK can of course also be due to differences in hydration of the two counterions.

There are several ways to test these conjectures. The inclusion of hydration water may be mimicked by different ionic radii. This effect was discussed above (cf. Table 2) and does not aid in explaining the experimental data. On the contrary, changing R_i from 2.0 to 3.0 Å for chloride ions decreases the pK shifts about 0.4 units, which increases even more the discrepancy between experimental and calculated values.

To test the effect of a high counterion polarizability, we added the following term to the Hamiltonian, eq 3:

$$u_a(r_{ij}) = -\frac{A_{ij}}{r_{ij}^4} \qquad (14)$$

where A_{ij} is an adjustable parameter. This parameter was chosen so that the interaction at contact contained an extra effective attractive energy ranging from −0.25 to −2.25 kT. As seen in Table 4, the polarizability term plays a significant role. Given a high extra attractive interaction of −2.25 kT between surfactants and counterions results in a decrease of 0.6 pK units.
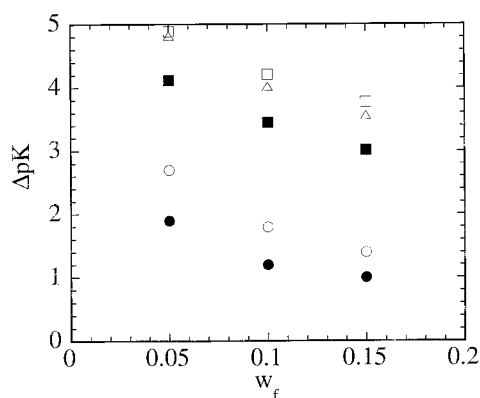
Figure 4. The difference in pK_a between anionic and cationic micelles vs the weight fraction of surfactant. Circles correspond to experimental values (●: DoTAB and ○: DoTAC). The rest of the symbols correspond to calculated ΔpK_a (□: Monte Carlo calculations with R_d = 0 Å; △: Poisson-Boltzmann calculations; and ■: Monte Carlo calculations with R_d = 18.67 Å. See text for details.).

So far, our discussion has been based on the assumption that pK_a^0 = pK_a^W. An alternative approach would be to consider two spherical micelles with the same radius and the same aggregation number, but with different surfactants, i.e., one negative and the other positive. Determining the apparent pK_a for lauric acid incorporated into each of them, and calculating ΔpK as pK_a^- − pK_a^+ eliminates the pK_a^0 determination issue. pK_a^- and pK_a^+ are the apparent pK_a determined in the anionic and cationic micelles, respectively. Results of such a procedure are presented in Figure 4. Even though the calculated values are larger than the experimentally determined ones, the agreement is fair, keeping in mind that we have not tried to optimize any of the parameters such as ionic radii, surface charge density, or micellar aggregation number. The concentration dependence is correctly predicted. Note also that in this comparison the uniform and nonuniform models predict comparable pK_a shifts, on account of cancellation effects as discussed above.

V. Conclusion

To theoretically model the addition or deletion of a unit charge is difficult. The solvation free energy of an ion in water is on the order of 1000 kJ/mol, while the experimental pK shifts of interest correspond to energies in the range 1−10 kJ/mol. When including a dielectric discontinuity we are in effect trying to calculate a huge desolvation energy and the accuracy needed is prohibitive. This is probably the main reason for the lack of good agreement between experiment and theory. Note, however, that the numbers calculated are in all cases of the correct order of magnitude, that is, a few kJ/mol. If, on the other hand, we are satisfied with relative differences, then the picture becomes more appealing: the effect of micelle concentration is properly reproduced. Here the dielectric continuum model is obviously doing an excellent job. Comparison between Monte Carlo and Poisson−Boltzmann results shows an almost quantitative agreement, although there is a difference between the two methods when a dielectric discontinuity is introduced.

Specific ion effects have been intensely debated and our experiments point to a possible difference between bromide and chloride as counterions. The polarizability of Br$^-$ is somewhat higher than that of Cl$^-$. To include the polarizability in a rigorous way in the simulations is difficult and time-consuming, but the inclusion of an effective attractive energy term in the Hamiltonian seems to produce a change in the correct direction.

It is interesting to compare the experimental and calculated ΔpK obtained in this study with those found in proteins. In

proteins close to the iso-electric point, one typically observes both positive and negative pK shifts depending on the local environment of the titrating group.[23,44] For highly charged protein, e.g., a negatively charged protein, a common observation is that lysine or other basic residues are upshifted.[38,45,46] A highly positive protein shows downshifted acidic groups,[16] which is opposite to what is found for the cationic micelles in this study.

References and Notes

(1) Mukerjee, P.; Banerjee, K. *J. Phys. Chem.* **1964**, *68*, 3567.

(2) Fernández, M. S.; Fromherz, P. *J. Phys. Chem.* **1977**, *81*, 1755.

(3) Lovelock, B.; Grieser, F.; Healy, T. W. *J. Phys. Chem.* **1985**, *89*, 2103.

(4) Drummond, C. J.; Grieser, F.; Healy, T. W. *J. Phys. Chem.* **1988**, *92*, 2604.

(5) Grieser, F.; Drummond, C. J. *J. Phys. Chem.* **1988**, *92*, 5580.

(6) Drummond, C. J.; Grieser, F. *Photochem. Photobiol.* **1987**, *45*, 19.

(7) Garcia-Soto, J.; Fernández, M. S. *Biochim. Biophys. Acta* **1983**, *731*, 275.

(8) Friedman, H. L. *Annu. Rev. Phys. Chem.* **1981**, *32*, 179.

(9) Hill, T. L. *Statistical Mechanics*; McGraw-Hill: New York, 1956.

(10) Jönsson, B. *The Thermodynamics of Ionic Amphiphilie-Water Systems − A Theoretical Analysis*, Ph.D. Thesis, Lund University, Lund, Sweden, 1981.

(11) Almgren, M.; Linse, P.; van der Auwerarer, M.; De Schryver, F. C.; Geladé, E.; Croonen, Y. *J. Phys. Chem.* **1984**, *88*, 289.

(12) González-Tovar, E.; Lozada-Cassou, M. *J. Phys. Chem.* **1989**, *93*, 3761.

(13) Linse, P.; Gunnarsson, G.; Jönsson, B. *J. Phys. Chem.* **1982**, *86*, 413.

(14) Linse, P.; Jönsson, B. *J. Chem. Phys.* **1983**, *78*, 3167.

(15) Linse, P. *J. Phys. Chem.* **1986**, *90*, 6821.

(16) Kesvatera, T.; Jönsson, B.; Thulin, E.; Linse, S. *Proteins: Struct., Func.,* Genetics **1999**, **1999**, *37*, 106.

(17) da Silva, F. L. B.; Jönsson, B.; Penfold, R. *Protein Science* **2001**, *10*, 1415.

(18) Harvey, S. C. *Proteins: Struct., Funct., Genet.* **1989**, *5*, 78.

(19) Bashford, D. *Curr. Opin. Struct. Biol.* **1991**, *1*, 175.

(20) Sharp, K. A. *Curr. Opin. Struct. Biol.* **1994**, *4*, 234.

(21) Warshel, A.; Åqvist, J. *Annu. Rev. Biophys. Biophys. Chem.* **1991**, *20*, 267.

(22) Sharp, K. A.; Nicholls, A.; Sridharan, S. *Delphi − A Macromolecular Electrostatics Modeling Package*. Columbia University, 1998.

(23) Antonsiewicz, J.; McCammon, J. A.; Gilson, M. K. *J. Mol. Biol.* **1994**, *238*, 415.

(24) Simonson, T.; Perahia, D. *J. Am. Chem. Soc.* **1995**, *117*, 7987.

(25) Simonson, T.; Brooks, C. L., III. *J. Am. Chem. Soc.* **1996**, *118*, 8452.

(26) Löffler, G.; Screiber, H.; Steinhauser, O. *J. Mol. Biol.* **1997**, *270*, 520.

(27) Smith, P. E.; et al. *J. Phys. Chem.* **1993**, *97*, 2009.

(28) Stigter, D. *J. Phys. Chem.* **1964**, *68*, 3603.

(29) Levesque, D.; Weis, J. J.; Hansen, J. P. Simulation of classical fluids. In *Monte Carlo Methods in Statistical Physics*; Binder, K., Ed.; Springer-Verlag: Berlin, 1986; Vol. 5, pp 47−119.

(30) Böttcher, C. J. F. *Theory of Electric Polarization*; Elsevier: Amsterdam, 1973.

(31) Metropolis, N. A.; Rosenbluth, A. W.; Rosenbluth, M. N.; Teller, A.; Teller, E. *J. Chem. Phys.* **1953**, *21*, 1087.

(32) Frenkel, D.; Smit, B. *Understanding Molecular Simulation: From Algorithms* to Applications; Academic Press: San Diego, 1996.

(33) Jönsson, B. *Poisson−Boltzmann cell program*. Available from http://www.membfound.lth.se/chemeng1.html.

(34) Svensson, B. R.; Woodward, C. E. *Mol. Phys.* **1988**, *64*, 247.

(35) van der Zegel, M.; Croonen, Y.; Geladé, E.; van der Auweraer, M.; Vandendriessche, H.; De Schryver, F. C.; Almgren, M. *J. Phys. Chem.* **1983**, *87*, 1426.

(36) Johansson, L. B.-Å.; Söderman, O. *J. Phys. Chem.* **1983**, *91*, 5275.

(37) Press, W. H.; Flannery, B. P.; Teukolsky, S. A.; Vetterling, W. T. *Numerical Recipes in FORTRAN 77*; Cambridge University Press: Cambridge, 1993.

(38) Kesvatera, T.; Jönsson, B.; Thulin, E.; Linse, S. *J. Mol. Biol.* **1996**, *259*, 828.

(39) Bunton, C. A.; Yatsimirsky, A. K. *Langmuir* **2000**, *16*, 5921.

(40) *CRC Handbook of Chemistry and Physics*, 55th ed.; Weast, R. C., Ed.; CRC Press: Boca Raton, FL, 1975.

(41) Small, D. M. *Physical Chemistry of Lipids from Alkanes to Phospholipids*, 2nd ed.; Plenum Press: New York, 1988.

(42) Spooner, P. J. R.; Clark, S. B.; Glantz, D. L.; Hamilton, J. A.; Small, D. M. *J. Biol. Chem.* **1988**, *263*, 1444.

(43) Pyper, N. C.; Pike, C. G.; Edwards, P. P. *Mol. Phys.* **1992**, *76*, 353.

(44) Antonsiewicz, J.; McCammon, J. A.; Gilson, M. K. *Biochemistry* **1994**, *35*, 7819.

(45) Zhang, M.; Vogel, H. J. *J. Biol. Chem.* **1993**, *268*, 22420.

(46) Zhang, M.; Thulin, E.; Vogel, H. J. *J. Prot. Chem.* **1994**, *13*, 527.